Observations

of the

OWENS VALLEY RADIO OBSERVATORY

California Institute of Technology

Pasadena, California

1964

5. ACCURATE RIGHT ASCENSIONS FOR 227 RADIO SOURCES

by

E. B. Fomalont, T. A. Matthews,
D. Morris and J. D. Wyndham

ACCURATE RIGHT ASCENSIONS FOR 227 RADIO SOURCES

by

E. B. Fomalont, T. A. Matthews, D. Morris and J. D. Wyndham

ABSTRACT

The two 90-foot steerable paraboloids of the Owens Valley Radio Observatory were used as an east-west interferometer to measure the right ascension of 227 radio sources. The observations were made between January, 1960, and July, 1961, at spacings of 195λ (958 Mc/s) and 283λ (1390 Mc/s). Corrections for resolution and known confusing sources have been evaluated. The standard errors for a source position range between 3 seconds of arc and 20 seconds of arc, with an average value of 9 seconds of arc.

I. INTRODUCTION

For some years the Owens Valley Radio Observatory has systematically measured the radio positions of a number of radio sources. The final goal of this program is to obtain identification of the radio sources with optical objects.

This paper is concerned only with the measurement of right ascension of 227 sources. For this purpose the two 90-foot steerable paraboloids were used as a two-element interferometer with a 200-foot east-west baseline. The observations were made in four separate series as indicated in Table 1. The sources chosen for observation varied throughout the different series. In the first series, the CTA list of sources (Harris and Roberts 1960), with a few additional fainter sources of interest, was used. However, it was realized from the observations of this first series that accurate positions could be obtained for much weaker sources. For this reason a new list of sources was compiled for the last three series of observations. This list included all sources in the 3C catalog (Edge, Shakeshaft, McAdam, Baldwin and Archer 1959) having $S_{159} \geq 14.5 \times 10^{-26}$ W m^{-2} (c/s)$^{-1}$. Occasionally a source was too weak to derive an accurate position and it was therefore omitted. In addition, sources from the Mills' catalogs (Mills, Slee and Hill 1958, 1960) were included for which Kellermann and Harris (1960) measured $S_{960} \geq 3 \times 10^{-26}$ W m^{-2} (c/s)$^{-1}$. Other sources from the CTA and CTB (Wilson and Bolton 1960) catalogs which were reasonably small in diameter were also included. This list gives fairly complete coverage of cataloged sources between declinations -45 and + 71

down to a flux level of $S_{960} = 4.5 \times 10^{-26}$ W m^{-2} (c/s)$^{-1}$.

Table 1

Date	Frequency	Spacing	Range of α	No. of Sources Observed
Jan.-March 1960	958 Mc/s	195λ	1^h - 17^h	77
June 1960	"	"	19^h - 10^h	87
Oct.-Nov. 1960	"	"	12^h - 23^h	123
July 1961	1390 Mc/s	283λ	17^h - 02^h	119

II. RECEIVER SYSTEM AND INTERFEROMETER RESPONSE

The operation of the two-element interferometer and the receiving equipment associated with it has been described in detail by Read (1963). The receiver at each antenna focus was of the superheterodyne type with a crystal mixer connected to the feed horn by a short length of cable. In the first two series of observations the local oscillator was common to both receivers, but subsequent to the middle of the third series the local oscillator power was produced by a klystron at each focus locked to a common reference oscillator as described by Read (1963). During the course of these and other minor changes, the phase stability of the system was measurably improved.

In an analysis of the interferometer response, Read (1963) has shown that the significant term of the recorder deflection is

$$\cos \left[2\pi D_\lambda \left(\sin \theta + \frac{x-y}{D}\right)\right] \qquad (1)$$

where D, D_λ = separation of antennas in units of length and units of wavelength, respectively;

θ = angle between source and the plane perpendicular to the antenna baseline;

x = difference in R. F. cable lengths between horns and mixers of the two antennas;

y = difference in L.O. cable lengths for the two antennas.

For a maximum in the interferometer response, the term in square brackets in expression (1) must equal $2\pi N$, where N is the lobe number counting from $\theta = 0$ and is held constant for a night's observations. Hence we may write

$$\sin \theta_N = \frac{N}{D_\lambda} - \frac{x-y}{D} \qquad (2)$$

where θ_N is the value of θ at the maximum of the Nth lobe.

For an east-west interferometer,

$$\sin \theta = d \sin \delta - (h'-H) \cos \delta \qquad (3)$$

where α, δ are the equatorial coordinates of the source.

d = declination of extended east-west baseline and is small.

h = hour angle of extended east-west baseline = $h' + \frac{\pi}{2}$, where h' is small.

H = hour angle of source = $t-\alpha$.

t = sidereal time.

Let T_N be the sidereal time measured for the maximum of the lobe nearest to meridian transit of the source. Substituting equation (3) into (2) gives

$$(\alpha-T_N) \cos \delta = E(t) - d \sin \delta + h' \cos \delta \qquad (4)$$

where

$$E(t) = \left(\frac{N}{D_\lambda} - \frac{x-y}{D}\right) .$$

Equation (4) is the basic equation used to derive the right ascension from the observations. The factors d and h' depend on the relative position of the bases of the antennas and are constants for a given series of observations. They are involved only as a function of the source declination. The term E(t), which is a function of the equipment phase, varies with time and does not repeat exactly from night to night.

III. OBSERVATIONAL PROCEDURE

Most of the observations were madeat night in order to avoid interference from the sun in the antenna sidelobes, and to reduce the effect of rapid temperature variations on the phase of the equipment. The few observations made in the daytime show these effects and have larger associated errors.

Each source was observed for about ten minutes centered about meridian transit. The times of about twenty crossovers in the interferometer fringe pattern were then used to provide an accurate value for the time of maximum nearest transit. The choice of the correct transit lobe was obvious in most cases from a comparison with the measured positions in other catalogs. However, for catalog positions where the errors are equal to or greater than one-half lobe, such as is sometimes the case for Mills' sources, the identi-

fication of the transit lobe was ambiguous. These ambiguities were eliminated by a special set of observations at a frequency of 1420 Mc/s using the primary beam of the antennas to identify the proper lobe, and all such sources are identified with a dagger in Table 3. All observations were corrected for clock errors and the effects of the receiver time constant. The positions were reduced to the epoch 1950 by correcting for the effects of general precession, nutation and aberration using Besselian star constants and day numbers.

IV. REDUCTION AND CALIBRATION

On any given night of observation during a series, transit times for thirty to forty sources were found. Included were a small number of sources of known optical counterpart, and the calibration technique used was to refer the measured radio positions to the optical positions of these identified radio sources.

Initially, the first series of observations was calibrated with respect to all of the then-identified sources. Many of these were of large radio diameter, which can introduce errors due to resolution effects, as well as possible errors due to displacements between the radio and optical centroids. In addition, the existing identifications were mainly in the northern hemisphere and equation (4) shows that the calibration sources should cover a large range of declinations in order to disentangle the quantities h', d and E(t). However, the resulting right ascensions, when combined with declination measures (from published lists, unpublished Cal Tech measurements and the accurate declinations of Read (1963)) enabled a number of new identifications to be made, many of which have been confirmed spectroscopically by M. Schmidt. From these identifications the sources in Table 2 were chosen to calibrate all four series of right ascension measurements discussed in this paper. The best calibration sources are those having small radio diameters (preferably no more than a few seconds of arc) and which also have small optical diameters. In column 4 of Table 2, the east-west size of the radio source is given to indicate the degree to which the source conforms to this criterion. The radio size is derived from the work of Moffet (1962), Maltby (1962) and Allen et al (1962). The assumption that the radio and optical positions coincide is discussed briefly in Section V (c).

On any one night of observation only a few of the calibration sources in Table 2 were observed, so that E(t) could not be derived with very great precision. A procedure was therefore used in which each night's observations in a series was reduced to a standard night using all the sources observed in common on both nights. This procedure had the additional advantage of allowing the final calibration to be done using average positions which had smaller associated errors than the positions determined from an individual night's observation. Thus assuming that d, h' remain constant since the antennas were not moved, and that the right ascensions for each source do not change from night to night, we can write for a single source

$$E(T_1) - E(T_2) = (T_1 - T_2) \cos \delta \qquad (5)$$

T_1 and T_2 being the transit times on nights 1 and 2, respectively. The quantity $E(T_1) - E(T_2)$ was formed for all sources observed in common on the two nights, plotted as a function of t, and a smooth mean curve drawn through the points. An example of such a curve is shown in Figure 2. This curve was then used to correct the values of T on night 2 to night 1. In a similar fashion, all other nights of a series were reduced to a single standard night.

All the calibrators observed in the entire series were used in equation (4) to determine the function E(t) and the constants d and h'. Writing $E(t) = E_o + E_1(t)$, the time varying part $[E_1(t)]$ was first determined using groups of calibration sources in small ranges of declination to restrict the effects of the terms containing d and h'. Having eliminated this first approximation for $E_1(t)$ from equation (4), the constants E_o, d, h' were found by a least squares method. These values were then used to redetermine the function $E_1(t)$ more accurately, after which a final determination of E_o, d, h' was made. Figures 3 and 4 show the final iteration used to derive E(t), d and h' for the July, 1961, series. The values of the constants are found from a least squares solution of equation (4).

V. SOURCES OF ERROR

The various sources of error are discussed below and are illustrated in Figures 1 to 5. In addition the magnitude of the system of errors has been checked by examining the differences between the positions from different series, and between the radio and optical positions, as compared to the quoted errors.

a) Receiver Noise Error, σ_r

The receiver noise produces an uncertainty, σ_r, in the value of T measured from the record. This uncertainty was determined for each observation and is plotted in Figure 1 for 958 Mc/s against the reciprocal intensity of the observed source. The effects of receiver noise are about 30% larger at 1390 Mc/s. This error is important only for sources having S_{958} less than about 5×10^{-26} W m-2 (c/s)-1. There was, in addition, a reading error from the chart records of 0.05 to 0.10 seconds of time.

b) Reduction to a Standard Night, σ_{co}

Figure 2 is a plot of $E(T_1)-E(T_2)$ for sources observed in common on the nights July 19-20 and July 18-19, 1960, versus the sidereal time. Vertical lines indicate the standard errors expected from the combination of the receiver noise errors on the two nights. The general shape of the curve is due to slow phase changes between the two receivers, the major portion of which is presumably due to changes in the lengths of the local oscillator

cables. The scatter about the mean line is greater than expected from the receiver noise alone. The additional scatter is attributed to random phase jumps in the receiver. For nights which had many sources in common (e.g. Figure 2), the error introduced from the comparison of nights, σ_{co}, is in the range 0.2 to 0.3 seconds of time at $\delta = 0$ for a single observation. In a few cases a lack of a sufficient number of common sources caused some additional uncertainty; in these cases σ_{co} was correspondingly increased.

c) Calibration Error

If the calibration curves are in error because of a lack of calibrators, then systematic errors will be introduced into the positions. The likelihood of such errors increases below declination -20°. A comparison between different series suggests that such systematic errors are small.

It has been tacitly assumed that the radio and optical positions of the calibrators are coincident. This assumption is partially confirmed by Figures 3 and 4 where the scatter around the two curves is that expected from the receiver noise and comparison error alone (see also Figures 6b and d). Because of the large number of calibrators present in the calibration curves, it seems likely that a significant random displacement of the radio from the optical position would appear as an increased scatter of points about the curves in Figures 3 and 4 no matter how judiciously the curves are chosen. In order to test this assumption, random displacements were introduced in the optical positions and the June 1960 series was re-reduced. The displacements were drawn from a gaussian distribution having a standard deviation of 1^{s}. The new equipment phase calibration curve and the new baseline calibration curve showed an increased scatter about the mean lines which reflected almost all of the 1^{s} scatter which was introduced. From this we conclude that the average displacement between the radio and optical positions for the sources in Table 2 is less than $0^{s}.5$.

d) Errors Due to Resolution

Phase shifts due to resolution by the interferometer cause changes in apparent position for many of the sources. In addition, if a source has a diameter comparable to the antenna pattern, then the measured position is sensitive to the antenna positions. Such sources are better left to a specialized set of observations or a higher primary resolution and have been omitted from the list of sources discussed in this paper.

The expected phase shift, and its associated error, due to resolution at 195λ (958 Mc/s) and 283λ (1390 Mc/s) for double sources has been calculated whenever possible using the model of the source given by Maltby and Moffet (1962). For sources whose structure is not double, the measured phase shift at 389λ (Moffet 1962), when available and less than 60°, has been used to find values at 283λ and 195λ by means of a cubic law (see Moffet 1962, equation 17). The results of these calculations are given in the notes to Table 3, and have been included in deriving the final positions in Table 4.

e) Errors Due to Confusion

The positional error introduced by confusion becomes serious at low flux values. This error may be conveniently separated into two parts: (i) confusion from one, or at most a few, nearby relatively-strong sources of known position and flux; and (ii) confusion from one or more unknown weak sources in the antenna pattern of each paraboloid.

(i) The phase shift caused by a relatively-strong nearby source, whose position and flux are known, on the position of the source under observation has been calculated. The source lists of PRRL (Foster 1961), 3C-R (Bennett 1962), 3C and MSH (Mills, Slee and Hill 1958, 1960) were searched for possible confusing sources. Additional information was taken from Scott and Ryle (1961) and from Kellermann (1963). The information is thought to be reasonably complete down to a flux level of $S_{958} = 1 \times 10^{-26}$ W m^{-2} (c/s)$^{-1}$ for declinations greater than zero. The results of the computations are given in the notes to Table 3, and the final positions in Table 4 include these corrections. Since any errors in the position and flux of the confusing source introduce further errors in the corrected position of the observed source, the standard error in Table 4 has been increased to take account of these uncertainties.

(ii) The average effects due to confusion by one or more unknown sources in the main antenna pattern of each paraboloid have been computed. The antenna pattern was represented by a circular gaussian having a half-power beam-width of 48' at 958 Mc/s. The number-flux relationship at 958 Mc/s (equation 6) was derived from the work of Scott, Ryle and Hewish (1961) using an average spectral index of -0.80, and is given by

$$N = 200\ S^{-1.80} \qquad \text{(at 958 Mc/s)}. \qquad (6)$$

Although the exponent agrees generally with an investigation by Kellermann and Read (1964) at 1421 Mc/s, the multiplicative constant found by the latter authors is somewhat larger, indicating that these confusion calculations are only approximate. For our computations we have used the numbers derived from the work of Scott, Ryle and Hewish (1961).

The calculation of the confusion probability follows the method developed by Scheuer (1957). Using this method, the probability, $P(\Delta\alpha)$, that a source of unit flux undergoes an apparent change in position by more than $\Delta\alpha$ seconds of time at the equator was computed, and the result is illustrated in Figure 5 (top curve). The bottom curve in Figure 5 gives the values of $P(\Delta\alpha)$ when the effects of sources having a flux greater than 1×10^{-26} W m^{-2} (c/s)$^{-1}$ at 958 Mc/s are eliminated.

Values of $P(\Delta\alpha)$ from Figure 5 can be compared with the average values of the standard errors for sources in Table 4. The comparison shows that for 10% of the sources having a flux of

6×10^{-26} W m^{-2} $(c/s)^{-1}$ at 958 Mc/s, the effect of confusion becomes equal to the average standard error.

f) The Error System

For every source in each series a standard error was computed from the rms combination of the receiver noise error and the comparison error and included any necessary adjustment for larger than normal uncertainties in the reduction procedure. The magnitude of the system of errors was checked by comparing the independent positions of the same source determined in different series of measurements. The frequency distribution of $\Delta\alpha/\sigma_d$ was examined, where $\Delta\alpha$ is the difference between the measured positions and σ_d is the expected error obtained by combining the errors of the two measurements. Care was taken to eliminate sources whose comparison would be influenced by known confusion and resolution effects. The frequency distributions for different combinations of the series were gaussians centered at zero as expected. Four sets of comparisons were made. 1) All possible comparisons between different series at 195λ separation. 2) All possible comparisons between 195λ positions in each series and the optical positions from Table 2. 3) All possible comparisons between 283λ positions and the positions in the individual 195λ series. 4) All possible comparisons between the 283λ positions and the optical positions. In each set of comparisons, the standard deviation of the distribution was computed in the normal manner. The results of the comparisons are displayed in Figure 6 where the absolute values of $\Delta\alpha/\sigma_d$ are plotted. The four values of $\sigma(\Delta\alpha/\sigma_d)$ are all close to unity, demonstrating that on the average the differences in position are those expected from the errors.

VI. TABULAR DATA

Table 3 lists separately the observed right ascensions for the two different spacings for 227 sources. The values for an antenna spacing of 195λ (958 Mc/s) are averages of the different series of observations. An asterisk in column 4 signifies that the source was observed in two different series at 195λ, no source being observed in all three series. The standard error of the average position was derived by averaging two independent estimates of the error, one estimate from the difference between the positions in the two series, the other from the errors of the individual positions. The notes to Table 3 give the phase shifts due to resolution and confusion, and in addition, comments about the source size when of interest. Sources without notes are believed to be unconfused and to have no phase shift due to resolution.

Table 4 is a list of final right ascensions for 197 radio sources. All sources which have no phase shift due to resolution and which are not confused are taken directly from Table 3, taking weighted averages of the 195λ and 283λ positions where applicable. Other sources with a small or well defined phase shift due to resolution or confusion are entered in Table 4 with the appropriate corrections made to the right ascension and its standard error.

For those sources observed at the two spacings the standard errors were derived as described for Table 3. In all such cases the numbers in column 4 refer to the notes following Table 3 which describe the corrections applied. Sources having large poorly-known phase shifts have not been included in Table 4.

VII. ACKNOWLEDGMENTS

We wish to thank A. T. Moffet for information on the structure of several sources prior to publication. The work in radio astronomy at the California Institute of Technology is supported by the United States Office of Naval Research under contract Nonr 220(19).

REFERENCES

Allen, L. R., Anderson, B., Conway, R. G., Palmer, H. P., Reddish, V. C. and Rowson, B. 1962, M.N., 124, 477.

Bennett, A. S. 1962, Mem. R.A.S., 68, 163.

Edge, D. O., Shakeshaft, J. R., McAdam, W. B., Baldwin, J. E. and Archer, S. 1959, Mem. R.A.S., 68, 37.

Foster, P. R. 1961, Ph.D. Thesis, University of Cambridge.

Griffin, R. F. 1963, A.J., 68, 421.

Harris, D. E. and Roberts, J. A. 1960, Pub. A.S.P., 72, 237.

Hazard, C. 1962, M.N., 126, 343.

Jennison, R. C. and Latham, V. 1959, M.N., 119, 174.

Kellermann, K. I. and Harris, D. E. 1960, Observations of the California Institute of Technology, No. 7.

Kellermann, K. I. 1964, A.J., 68, 205.

Kellermann, K. I. and Read, R. B. 1964, in preparation.

Lequeux, J. 1962, Compte Rendue, 255, 1865.

Leslie, P.R.R. and Elsmore, B. 1961, The Observatory, 81, 14.

Maltby, P. 1962, Ap. J. Suppl., 7, 124.

Maltby, P. and Moffet, A. T. 1962, Ap. J. Suppl., 7, 141.

Mills, B. Y., Slee, O. B. and Hill, E. R. 1958, Aust. J. Phys., 11,360.

_____. 1960, Aust. J. Phys., 13,676.

Moffet, A. T. 1962, Ap. J. Suppl., 7, 93.

Read, R. B. 1963, Ap. J., 38, 1.

Scheuer, P. A. G. 1957, Proc. Camb. Phil. Soc., 53, 764.

Scott, P. F., Ryle, M. and Hewish, A. 1961, M.N., 122, 95.

Scott, P. F. and Ryle, M. 1961, M.N., 122, 389.

Wilson, R. W. and Bolton, J. G. 1960, Pub. A.S.P., 72, 331.

Table 2

OPTICAL RIGHT ASCENSIONS FOR CALIBRATION SOURCES

Source	α Optical	Radio Size (EW)	Remarks
3C 18	$00^h38^m14^s.2$	~15"	Identification not confirmed.
3C 26	00 51 34.9	< 0!7	
3C 28	00 53 08.86	~15"	
3C 43	01 27 15.04	< 1!0	Identification highly probable, but not confirmed.
3C 48	01 34 49.82*	< 1"	
3C 63	02 18 22.19	<15"	
3C 71	02 40 07.10*	<15"	
3C 78	03 05 49.07*	1!0	
3C 79	03 07 10.97	1!2	
3C 84	03 16 29.4	~15"	Halo ~20', core has ~80% of flux at 958 Mc/s. Can be confused by 3C 83.1.
3C 88	03 25 18.77	2'-3'	
MO4-12	04 05 30.61	(0!8)	NS diameter. Identification highly probable, but not confirmed.
3C 147	05 38 43.53*	~ 1"5	
3C 171	06 51 11.22	<30"	
3C 195	08 06 29.97	(1!5)	NS diameter. Probably ~50" EW.
3C 196	08 09 59.39*	< 1"	
3C 198	08 19 52.07	3!5	Halo has 75% of flux. Core <1!5 in diameter.
3C 212	08 55 55.8	<15"	Radio position from occultation (Hazard 1962).
CTB 31	08 57 21.6	1!8	Core has 35% of flux. Halo ≈10' in diameter.
3C 216	09 06 17.75	~ 3"	
3C 218	09 15 41.18*	42"	Core has 88% of flux. Halo ~5' in diameter.
3C 234	09 58 57.42*	< 1!0	60% of flux has a diameter of <1!0. Overall size, 3!0.
3C 254	11 11 54.41	< 4"	Not certain.
3C 272.1	12 22 31.48	(1!8)	NS diameter.
3C 273	12 26 32.44 12 26 33.35	14"	End of jet. Star-like object. Radio position depends on frequency.
3C 277.3	12 51 46.29*	40"	
3C 278	12 51 58.56* 12 51 59.44*	2!5	Simple radio structure.
3C 286	13 28 50.74*	20"	Halo has 60% of flux. Core <1".
3C 295	14 09 33.45*	3"	
3C 298	14 16 38.58*	2"3	Identification not certain.
3C 310	15 02 46.94* 15 02 48.14*	1!8	Radio double in P.A. 0°.
3C 315	15 11 30.82* 15 11 30.78*	1!0	Simple radio structure.
3C 317	15 14 17.00*	~20"	
3C 338	16 26 55.38*	1!2	Simple radio structure.

Table 2 (continued)

Source	α Optical	Radio Size (EW)	Remarks
3C 386	$18^h36^m12^s.85$*	1!9	Simple radio structure.
3C 388	18 42 35.44*	~15"	Confused?
3C 405	19 37 44.35*	1!5	Double in P.A. 109°.
	19 37 44.52*		
3C 430	21 17 03.7	0!6	
3C 433	21 21 30.50*		
	21 21 30.82*	~10"	
3C 436	21 41 57.0	~15"	Not confirmed.
3C 442	22 12 18.50*	(3')	NS diameter. Simple radio structure.
	22 12 20.40*		
3C 445	22 21 14.76*	1!6	Double in P.A. 0°.
3C 459	23 14 02.6	~ 2"	
M23-112	23 22 43.72*	~ 7"	

*Optical positions measured by Griffin (1963).

Table 3

MEASURED RIGHT ASCENSIONS

Source	α(1950.0) D = 195λ	Std. Error	No. of Obs.	α(1950.0) D = 283λ	Std. Error	No. of Obs.	Remarks
3C 2	$00^h03^m47^s.7$	±0.7	1	$00^h03^m49^s.1$	±0.6	3	
3C 5				00 09 47.6	0.9	3	
M00-29	00 21 59.7	0.6	1	00 22 00.0	1.0	1	
3C 10	00 22 30.3	0.6	4	00 22 32.9	1.1	3	(1)
3C 15	00 34 29.4	0.5	1	00 34 30.2	0.5	2	
3C 17	00 35 45.0	1.2	1	00 35 46.7	0.5	2	
3C 18	00 38 12.0	0.5	2	00 38 13.7	0.6	1	
3C 19				00 38 12.4	0.7	3	
M00-410	00 39 45.1	0.9	1	00 39 44.8	1.1	1	
3C 20	00 40 17.8	0.7	2				
M00-411	00 43 54.0	0.9	2	00 43 54.1	1.1	1	(2)
M00-222	00 45 08.7	0.9	1	00 45 05.1	0.7	1	(3)
3C 23	00 49 08.7	0.6	1	00 49 07.7	1.1	1	
3C 26	00 51 35.3	0.6	6*				
3C 27	00 52 41.4	0.9	2	00 52 40.8	1.5	1	
3C 28				00 53 09.4	0.9	1	
3C 29	00 54 58.4	0.5	1	00 55 00.6	0.8	3	(4)
M01-41	01 03 05.4	0.9	1	01 03 04.6	1.0	1	
3C 32	01 05 48.3	0.5	3				
3C 33	01 06 12.6	0.3	7*	01 06 13.9	0.4	6	
3C 34	01 07 33.0	0.6	2				(5)
3C 38	01 17 59.5	1.4	3*				
3C 40	01 23 25.3	0.7	8*				(6)
3C 41	01 23 51.9	0.5	1	01 23 55.1	0.7	2	(7)
3C 43	01 27 13.5	0.5	1	01 27 14.1	0.7	2	
3C 46	01 32 30.9	0.5	1	01 32 34.3	1.0	2	
3C 47	01 33 38.6	0.8	1	01 33 41.0	0.5	2	
3C 48	01 34 49.2	0.5	5*	01 34 49.3	0.5	5	
3C 55	01 54 18.3	0.5	2				
M01-315	01 57 58.4	0.6	2				
3C 58	02 01 47.3	0.5	6*				(8)
3C 62	02 13 13.3	0.5	2				(9)
3C 63	02 18 22.1	0.4	2*				
3C 66	02 19 57.7	0.6	10*				(10)
3C 65	02 20 30.2	0.6	1				(11)
3C 69	02 34 15.8	0.7	2				
M02-110	02 35 24.7	0.5	2				
3C 71	02 40 07.3	0.3	11*				
3C 75	02 55 04.4	0.6	12*				
3C 78	03 05 49.0	0.4	5*				

Table 3 (continued)

Source	α(1950.0) D = 195λ	Std. Error	No. of Obs.	α(1950.0) D = 283λ	Std. Error	No. of Obs.	Remarks
3C 79	$03^h07^m11^s.6$	±0.9	2*				
CTA 21	03 16 09.2	0.4	4*				
3C 84	03 16 29.2	0.4	16*				Per A (12)
3C 86	03 23 33.7	1.1	3*				
3C 88	03 25 18.7	0.5	2				
3C 89	03 31 42.0	0.4	2*				(13)
CTA 26	03 36 53.6	0.5	1				
M03-19	03 49 09.9	0.5	3				
M03-212	03 49 33.4	0.8	3				
3C 98	03 56 11.7	0.3	10*				
3C 99	03 58 31.6	0.5	1				
3C 103	04 04 35.7	0.8	2				
3C 105	04 04 45.0	0.5	2				(14)
M04-12	04 05 30.6	1.2	3				
3C 109	04 10 55.7	0.5	4				
M04-24	04 13 54.9	0.5	2				
3C 111	04 15 02.1	0.7	4*				
3C 119	04 29 07.8	0.5	2				
M04-112	04 31 51.4	0.5	2				
3C 123	04 33 55.6	0.4	3*				
M04-218	04 42 37.7	0.5	4				
3C 129	04 45 19.9	0.6	2				(15)
3C 131	04 50 11.8	0.5	2				(16)
3C 132	04 53 42.6	0.8	2				(17)
3C 133	04 59 53.7	0.6	1				
3C 134	05 01 18.2	0.7	4*				
M05-42+	05 11 31.4	1.0	1				
3C 135	05 11 34.2	0.9	2				(18)
3C 138	05 18 16.3	0.5	1				
M05-43	05 18 19.5	1.1	2				Pic A (19)
M05-36	05 21 12.4	0.7	4				
3C 144	05 31 30.5	0.3	21*				Tau A
3C 145	05 32 51.5	0.6	4				Ori A
3C 147	05 38 43.2	0.6	4*				
3C 149+	05 47 58.3	0.6	2				
3C 152+	06 01 27.7	0.6	1				
3C 153	06 05 43.4	0.6	3				
3C 154	06 10 42.8	0.6	8*				
3C 158	06 18 51.0	0.5	2				
3C 159	06 21 41.2	0.7	1				(20)

Table 3 (continued)

Source	α(1950.0) D = 195λ	Std. Error	No. of Obs.	α(1950.0) D = 283λ	Std. Error	No. of Obs.	Remarks
3C 161	$06^h24^m43^s.1$	±0.7	7*				
3C 166	06 42 24.7	0.5	2				
3C 171	06 51 11.7	0.8	6*				
M06-216	06 56 53.0	0.7	4				
3C 172	06 59 03.2	0.5	2				
3C 175	07 10 14.7	0.4	3*				
3C 178	07 22 31.7	0.6	3				(21)
3C 180	07 24 33.2	0.4	3				
2C 665+	07 31 22.6	0.7	1				PRRL 358
2C 676+	07 36 43.0	0.9	2				(22)
M07-117	07 45 16.3	0.5	4				(23)
3C 191	08 02 01.9	1.2	3*				
3C 192	08 02 35.6	0.5	2				
3C 195	08 06 30.6	0.5	3				(21)
3C 196	08 10 00.1	0.5	9*				
3C 198	08 19 52.6	0.6	3*				(24)
3C 200	08 24 18.6	0.6	1				
3C 202	08 31 56.8	0.9	5				(25)
3C 208	08 50 26.9	0.8	2				(26)
3C 212	08 55 55.0	0.8	3				
M08-47	08 57 23.0	1.0	1				(27)
CTB 32	08 57 41.4	1.0	1				(28)
M08-219	08 59 38.2	0.7	1				
3C 216	09 06 17.6	1.0	2*				
3C 218	09 15 42.1	0.4	26*				Hya A (29)
3C 219	09 17 51.5	0.8	1				
3C 222	09 33 51.5	1.2	1				
3C 225	09 39 31.1	0.5	3				(30)
3C 227	09 45 09.4	1.0	3*				
3C 228	09 47 28.3	0.6	1				
3C 230	09 49 24.0	0.7	1				
3C 231				$09^h51^m45^s.2$	±1.5	1	(31)
3C 234	09 58 57.3	0.7	3*				
3C 237	10 05 18.6	0.9	1				
3C 238	10 08 24.9	0.7	1				
3C 254	11 11 54.8	1.2	2				
3C 264	11 42 32.3	0.9	3				(32)
3C 265	11 42 53.4	0.6	3				
3C 270	12 16 49.9	0.4	6				(33)
3C 272.1				12 22 33.0	0.6	2	

Table 3 (continued)

Source	α(1950.0) D = 195λ	Std. Error	No. of Obs.	α(1950.0) D = 283λ	Std. Error	No. of Obs.	Remarks
3C 273	$12^h26^m33^s.8$	±0.3	2*	$12^h26^m33^s.5$	±0.5	2	
3C 274	12 28 16.1	0.5	21*	12 28 18.4	0.5	5	Vir A (34)
3C 275	12 39 45.0	0.4	3				
3C 277.3	12 51 47.4	0.7	2*	12 51 46.4	0.7	3	Com A
3C 278	12 51 59.3	0.3	9*	12 52 00.2	0.6	1	(35)
3C 279	12 53 35.9	0.8	2*				
3C 280	12 54 40.1	0.7	3				
3C 283	13 08 57.4	0.4	6*				
M13-42	13 22 35.2	0.6	7*	13 22 38.4	0.7	4	Cen A (36)
3C 287	13 28 15.0	0.4	2*	13 28 15.0	0.5	1	(37)
3C 286	13 28 49.7	0.5	4				
M13-011	13 35 30.1	0.5	2	13 35 35.5	0.6	1	(38)
3C 295	14 09 33.1	0.4	15*	14 09 33.4	0.7	5	
3C 298	14 16 38.5	0.5	4	14 16 39.3	0.8	2	
3C 300.1+	14 25 58.3	0.5	3				(39)
M14+010	14 34 29.5	0.6	1	14 34 26.6	1.5	3	(40)
M14-121	14 53 13.1	0.6	1	14 53 12.5	0.5	2	
3C 309.1+				14 58 53.0	1.1	2	
3C 310	15 02 48.4	0.4	12*	15 02 48.6	0.6	1	(41)
3C 313	15 08 33.0	0.4	2*	15 08 33.2	0.5	1	
3C 315	15 11 31.0	0.4	5*	15 11 30.6	0.8	4	
3C 317	15 14 18.9	0.9	5	15 14 17.6	0.8	1	
3C 318	15 17 50.0	0.5	3*	15 17 50.1	0.7	1	
3C 319	15 22 43.0	1.1	1	15 22 46.0	0.8	3	
M15-43+	15 26 52.2	1.0	1	15 26 55.2	0.9	2	(42)
3C 321				15 29 39.0	0.6	1	
3C 324	15 47 37.7	0.6	4*	15 47 37.2	0.6	1	(43)
3C 327	15 59 55.5	0.5	4*	15 59 57.1	0.3	6	(44)
3C 327.1	16 02 13.4	0.7	4*				
M16+03				16 03 39.5	0.6	2	
3C 330	16 09 15.1	0.9	2*				
3C 332	16 15 46.8	0.7	1	16 15 45.1	0.8	3	
3C 334				16 18 07.5	0.7	2	
M16-18	16 21 13.3	0.5	1	16 21 13.8	1.0	1	
3C 338	16 26 55.0	0.5	5*	16 26 54.1	0.7	4	
M16-47+	16 37 10.9	0.7	2	16 37 06.5	1.5	2	(45)
3C 345	16 41 19.6	0.8	1	16 41 17.1	0.9	2	
3C 347	16 43 25.7	0.5	1	16 43 10.1	1.3	2	(46)
3C 348	16 48 41.3	0.3	19*	16 48 41.0	0.5	6	Her A
3C 353	17 17 56.7	0.3	7*	17 17 55.7	0.4	3	

Table 3 (continued)

Source	α(1950.0) D = 195λ	Std. Error	No. of Obs.	α(1950.0) D = 283λ	Std. Error	No. of Obs.	Remarks
M17-34	$17^h20^m04^s.5$	±0.8	1	$17^h20^m00^s.9$	±1.4	2	(45)
M17-37+				17 27 05.1	0.8	3	(22)
3C 358	17 27 43.0	0.6	3*	17 27 40.5	0.7	2	Kepler S.N.
M17-39+				17 37 04.6	0.7	3	(22)
M17-213	17 42 32.5	0.4	7	17 42 31.9	0.5	5	Sgr A (47)
M17-114+	17 55 50.1	0.5	2				(22)
3C 365	17 56 11.2	0.8	1	17 56 14.0	0.8	1	(48)
M17-217				18 00 07.1	0.7	3	
M18-13	18 11 16.7	0.5	2	18 11 17.4	0.6	1	(49)
M18-33+				18 17 07.4	1.2	2	
CTB 52	18 17 39.9	0.5	5	18 17 37.5	0.5	3	M 17 (50)
M18-19+				18 25 33.4	0.9	2	(22)
3C 380	18 28 12.9	0.5	2	18 28 11.1	0.8	1	
3C 382	18 33 12.3	0.5	1	18 33 12.9	0.7	1	
3C 386	18 36 13.6	0.5	1	18 36 13.2	0.7	1	
3C 387+				18 38 01.3	0.8	2	(51)
3C 388	18 42 36.3	0.7	1	18 42 35.4	0.9	1	(52)
3C 390				18 43 15.2	0.5	2	
3C 389	18 43 44.1	0.9	1	18 43 45.2	0.5	2	(53)
3C 391	18 46 51.4	0.5	1	18 46 47.2	0.7	1	(54)
3C 394	18 57 04.7	0.6	2	18 57 05.2	0.7	2	
3C 396				19 01 36.5	0.5	4	(55)
3C 397	19 05 05.0	0.5	1	19 05 09.0	0.6	4	(56)
M19-46	19 32 17.8	0.9	1	19 32 17.5	1.0	2	
M19-111	19 38 26.5	0.5	1	19 38 23.1	0.5	2	(57)
3C 401	19 39 37.8	1.2	4*	19 39 38.2	0.9	2	
3C 402	19 40 22.8	0.7	2	19 40 22.2	0.9	1	
3C 403	19 49 43.2	0.5	2	19 49 44.0	0.8	2	
3C 405	19 57 44.7	0.4	15*	19 57 44.2	0.5	7	Cyg A
3C 409	20 12 18.0	0.8	3*				
CTB 87	20 14 10.0	0.5	2	20 14 11.3	0.7	1	(58)
3C 410	20 18 03.9	0.5	5*				
3C 413	20 28 25.0	1.0	1				
M20-37				20 32 35.6	0.5	3	
3C 418	20 37 06.6	0.4	6*				
3C 424	20 45 44.2	0.5	2	20 45 44.7	0.7	2	
M20-214	20 53 15.7	1.2	2	20 53 12.4	0.5	3	(59)
M20-215	20 58 37.7	0.7	2	20 58 40.6	0.7	1	(60)
M21-21	21 04 26.1	0.5	4*				(61)
3C 427.1				21 04 41.7	3.1	3	

Table 3 (concluded)

Source	α(1950.0) D = 195λ	Std. Error	No. of Obs.	α(1950.0) D = 283λ	Std. Error	No. of Obs.	Remarks
3C 428	$21^h06^m42^s.0$	±0.7	2*				(62)
3C 430	21 17 02.9	1.0	3*				
3C 431	21 17 09.0	0.8	3*				
3C 433	21 21 30.7	0.5	7*	$21^h21^m30^s.5$	±0.5	6	
3C 435	21 26 38.0	0.8	1				
M21-47	21 40 26.8	1.3	2	21 40 22.6	1.0	2	(45)
3C 436	21 41 57.8	0.8	2	21 41 57.4	0.7	2	
3C 437	21 45 00.0	0.7	3*				
CTA 97	21 51 32.4	1.8	2	21 51 36.3	1.0	2	(63)
3C 438	21 53 45.8	0.5	4*				
3C 441	22 03 50.3	0.7	2	22 03 49.7	0.8	3	
3C 444	22 11 43.0	0.5	5*				
3C 442	22 12 20.4	0.7	6*				
3C 445	22 21 15.3	0.5	8*	22 21 15.5	0.5	3	
3C 446	22 23 11.8	0.3	5*	22 23 10.6	0.5	1	
CTA 102	22 30 07.1	0.4	3*	22 30 08.1	0.7	1	
3C 452	22 43 29.7	0.6	9*				(64)
M22-46	22 50 10.2	0.9	3				
3C 455	22 52 37.2	0.6	1	22 52 35.4	0.8	2	
3C 456	23 09 55.4	0.4	2*	23 09 55.9	1.0	1	
3C 459	23 14 02.5	0.5	1	23 14 02.1	0.6	4	
3C 461	23 21 06.3	0.5	18*	23 21 07.8	0.9	3	Cas A (65)
M23-112				23 22 43.3	0.8	2	
M23-43				23 23 51.8	0.9	1	(22)
M23-44				23 31 42.8	0.8	2	
3C 465	23 35 56.0	0.6	6	23 35 57.2	0.6	3	(66)

Notes to Table 3

In these notes the convention has been adopted that a positive phase shift leads to an increase in the apparent right ascension of the source. $\Delta\alpha$ is the magnitude and direction of the change in position of the source caused by the phase shift due to resolution and/or confusion by nearby sources. For several sources it was necessary to take a drift curve, using the interferometer at a spacing of 283λ, to determine the proper lobe of the interferometer pattern. These sources are indicated by a dagger (†) in the first column. Those sources which have an asterisk (*) in the fourth column were observed in two of the different series of observations made at 195λ (958 Mc/s). The following abbreviations are made in the notes: ATM = Moffet (1962), PM = Maltby (1962), M^2 = Maltby and Moffet (1962), 3C = Edge et al (1959), 3C-R = Bennett (1962), PRRL = Foster (1961), MSH = Mills et al (1958 or 1960), CTB = Wilson (1963), ERL = Elsmore et al (1959), K = Kellermann (1964).

(1) 3C 10. Ring shaped source of diameter 6!5. The model given by M^2, when the 195λ and 283λ positions are incorporated, predicts a $\Delta\alpha = +2^s.3 \pm 1^s.0$ at 195λ, and $\Delta\alpha = +4^s.7 \pm 2^s.0$ at 283λ. This interpretation agrees well with the 3C position at 308λ and the ERL position at 465λ.

(2) M00-411. MSH says the diameter is >40". However, the agreement between the positions at 195λ and 283λ suggest that there is little or no phase shift.

(3) M00-222. East-west size about 3' (M^2). The disagreement between the positions at the two spacings suggest a phase shift due to resolution is present, mainly in the 283λ position.

(4) 3C 29. Diameter < 3!0 (3C-R). M^2 gives a diameter of 2!5 ± 0!7 (NS). A small phase shift (< 4°) due to resolution is possible.

(5) 3C 34. Confused slightly by 3C 31 (3C-R), resulting in a shift in position of $\Delta\alpha = -0^s.3 \pm 0^s.3$ at 195λ.

(6) 3C 40. According to the model of M^2, the phase shift due to resolution is $\Delta\alpha = +0^s.9 \pm 0^s.6$ at 195λ.

(7) 3C 41. Confused by PRRL 78, $\alpha = 01^h25^m12^s.1$ ($\pm 2^s$ est), $\delta = +32°26!6$ (±3' est), flux = 40% of 3C 41 (K). This produces a $\Delta\alpha = -0^s.9 \pm 0^s.4$ at 195λ, and a $\Delta\alpha = +0^s.3 \pm 0^s.2$ at 283λ. Complex source with large-scale structure (M^2). The effects of resolution are not known, but appear to be significant from a comparison of the positions at 195λ and 283λ.

(8) 3C 58. Large galactic source having an east-west diameter of 6!0 ± 1!0 (M^2). A significant but unknown phase shift due to resolution is likely.

(9) 3C 62. A wide north-south double source with an 11' separation in P.A. = 0° (M^2). The east-west size is unknown, but is probably small producing little phase shift at 195λ.

Notes to Table 3 (continued)

(10) 3C 66. According to the model of M^2, the phase shift due to resolution is $\Delta\alpha = +2^s.0 \pm 1^s.3$ at 195λ.

(11) 3C 65. East-west size is 3!7 ± 1!0 (3C-R). The 3C-R position suggests there may be a small positive phase shift at 195λ.

(12) 3C 84. The position of 3C 83.1 given by Leslie and Elsmore (1961) is one lobe spacing (17!7) in right ascension away from 3C 84. The resulting shift in position of 3C 84 is $\Delta\alpha = 0^s.0 \pm 0^s.2$.

(13) 3C 89. The structure is ambiguous. Either an east-west double of separation 6' of unknown intensity ratio, or a 10' halo with a small core displaced from the center. Due to the uncertainty in the model the phase shift at 195λ is unknown (private communication ATM).

(14) 3C 105. The radio structure is a halo of diameter 5!0 ± 1!0 with 50% of the flux, and a core of diameter >1!0 (M^2). There is probably little or no phase shift due to resolution at 195λ (ATM).

(15) 3C 129. Complex source of east-west diameter ~6' (M^2), producing an unknown phase shift at 195λ due to resolution.

(16) 3C 131. Confused by a source at $\alpha = 04^h49^m18^s$ ($\pm 2^s$ est), $\delta = +31^\circ54'$ ($\pm 3'$ est), flux = 30% of 3C 131 (K) which produces a $\Delta\alpha = +0^s.7 \pm 0^s.5$ at 195λ. The source is <0!6 north-south (M^2), but the east-west size is unknown. There is probably no phase shift due to resolution.

(17) 3C 132. Confused by a source at $\alpha = 04^h52^m26^s$ ($\pm 2^s$ est), $\delta = +23^\circ06'$ ($\pm 3'$ est), flux = 30% of 3C 132 which produces a $\Delta\alpha = 0^s.0 \pm 0^s.4$ at 195λ.

(18) 3C 135. Complex source of diameter ≥4', with fine structure <1!0 (M^2). Using the phase measured by ATM for 389λ it is estimated that $\Delta\alpha = +0^s.8 \pm 0^s.5$ at 195λ.

(19) M05-43. The east-west diameter is 7!5 ± 1!0 (M^2). There is a phase shift of $-120^\circ \pm 20^\circ$ at 389λ (ATM), thus the phase shift due to resolution cannot be estimated at 195λ.

(20) 3C 159. Confused by a source at $\alpha = 06^h21^m50^s$ ($\pm 2^s$ est), $\delta = +40^\circ30'$ ($\pm 3'$ est), flux = 27% of 3C 159 (K). This produces a $\Delta\alpha = +1^s.3 \pm 0^s.8$ at 195λ. Unresolved north-south (PM), and probably no appreciable east-west phase shift due to resolution at 195λ.

(21) 3C 178, 3C 195. Unresolved north-south (PM), and probably no appreciable phase shift due to resoltuion east-west at 195λ.

(22) 2C 676, M17-37, M17-39, M17-114, M18-19, M23-43. No size information available.

(23) M07-117. Complex source of diameter > 3' north-south, with fine structure < 1' (M^2). East-west size and phase shift due to resolution unknown.

(24) 3C 198. The radio structure consists of a core < 1!5, and a circular halo of 3!5 ± 1!0 having 75% of the flux (M^2). No phase shift due to resolution at 195λ (ATM).

(25) 3C 202. Not resolved north-south (PM); however, PRRL gives an east-west size of 4'. The positions for 3C 201 and 3C 202 in 3C and PRRL do not make sense. There may be a phase shift at 195λ.

(26) 3C 208. The radio structure of 3C 208 given by M^2 is incorrect due to the confusion from 3C 208.1. East-west structure of 3C 208 is unknown (private communication ATM). No corrections can be made for 3C 208.1 since its position is very poorly determined (3C-R).

(27) M08-47 = CTB 31. Galactic source with core diameter 1!8 ± 0!4, and halo diameter ≈10' having approximately 65% of the flux (M^2). The phase shift at 195λ could be $\Delta\alpha = -0^s.5 \pm 0^s.5$ according to the phase shift measured at 389λ (ATM), however, we have assumed a zero phase shift in Table 4.

(28) CTB 32. The radio diameter is 1!4 ± 0!4 (M^2). No phase shift due to resolution at 195λ.

(29) 3C 218. The radio structure consists of a core of diameter < 0!6 east-west having 90% of the flux, and a 5' halo (M^2). Based on the measured phase shift at 389λ (ATM), $\Delta\alpha = +0^s.3 \pm 0^s.3$ at 195λ.

(30) 3C 225. East-west structure unknown. Suspected wide double of ~12' north-south, causing an unknown east-west phase shift (private communication ATM).

(31) 3C 231. The radio diameter is 42" (Lequeux 1963).

(32) 3C 264. The radio structure consists of a core of diameter < 1!2 with 60% of the flux, and a halo of approximately 5' in diameter (M^2). There is no phase shift at 195λ (ATM).

(33) 3C 270. A near-equal radio double with an east-west separation 4!7 ± 0!3 (M^2), but producing no phase shift at 195λ.

(34) 3C 274. The radio structure consists of a halo 6!5 ± 0!7 in diameter with 48% of the flux at 958 Mc/s, and a core of 0!6 ± 0!2 diameter. At 195λ and 283λ the halo is partly resolved and thus a phase shift may be introduced as is suggested by the disagreement between the 195λ and 283λ positions. The 283λ position should be close to the core position, and it is therefore given in Table 4.

(35) 3C 278. Almost circular source of diameter 2!0 ± 0!5. From the measured phase shift at 389λ (ATM) it is estimated that $\Delta\alpha = +0^s.6 \pm 0^s.4$ at 195λ, and $\Delta\alpha = +1^s.3 \pm 0^s.8$ at 283λ.

(36) M13-42. The phase shift due to resolution at 195λ is $\Delta\alpha = +0^s.3 \pm 0^s.2$, and at 283λ is $\Delta\alpha = +3^s.7 \pm 1^s.7$ as calculated from the model of M^2.

(37) 3C 287. Confused by a source at $\alpha = 13^h28^m58^s$ ($\pm 2^s$ est), $\delta = +25^\circ05'$ ($\pm 3'$ est), flux = 40% of 3C 287 (K) which produces a $\Delta\alpha = -0^s.8 \pm 0^s.3$ at 195λ, and a $\Delta\alpha = -0^s.5 \pm 0^s.3$ at 283λ.

(38) M13-011. Unresolved north-south (PM); however, the disagreement between the positions at 195λ and 283λ suggests an east-west phase shift at both frequencies.

(39) 3C 300.1 = M14-011. Possible large-scale structure (M^2), but PRRL suggests it is small. The phase shift is assumed to be zero.

(40) M14+010. Confused by a source at $\alpha = 14^h35^m51^s$ ($\pm 2^s$ est), $\delta = +03^\circ58'$ ($\pm 3'$ est), flux is 60% of M14+010 (K), which produces a $\Delta\alpha = +2^s.0 \pm 1^s.0$ at 195λ, and a $\Delta\alpha = -1^s.2 \pm 0^s.5$ at 283λ. Large-scale structure present (M^2), but the phase shift east-west is small (ATM). PRRL found an extended source at this position (Bennett and Smith 1961).

(41) 3C 310. Two components with a separation in P.A. = 0 of 2!1 ± 0!2. No east-west phase shift due to resolution.

(42) M15-43. No size information available, but the disagreement between the 195λ and 283λ positions suggests that some phase shifts may be present.

(43) 3C 324. Confused by 3C 323.1 which produces a $\Delta\alpha = -0^s.8 \pm 0^s.3$ at 195λ, and has a negligible effect at 283λ.

(44) 3C 327. The phase shift due to resolution is $\Delta\alpha = +0^s.4 \pm 0^s.2$ at 195λ, and $\Delta\alpha = +0^s.9 \pm 0^s.4$ at 283λ as computed from the model of M^2.

(45) M16-47, M17-34, M21-47. MSH says the radio diameter is >45". The disagreement between the 195λ and 283λ positions indicate large east-west phase shifts are present.

(46) 3C 347. Recent observations suggest a wide double with a separation of ≈15' leading to large phase shifts at 195λ and 283λ (private communication ATM).

(47) M17-213. The radio structure consists of a core of diameter 2!2 ± 0!5, and a halo of diameter ~12' having 80% of the flux (M^2). No east-west phase shift at 195λ and 283λ (ATM).

Notes to Table 3 (continued)

(48) 3C 365. The positions given here agree with the 3C positions when the latter are corrected by +1 δ lobe and -1 α lobe.

(49) M18-13. Size unknown, but agreement between the 195λ and 283λ positions indicate little or no phase shift.

(50) CTB 52. There appears to be a significant phase shift due to resolution between the 195λ and 283λ positions. The direction is consistent with the phase measurements of ATM which suggest that there is a small component of the source at $\alpha = 18^h17^m35^s$. Our measurements when extrapolated to zero spacing by the cubic law suggest that $\Delta\alpha = -2^s.2 \pm 0^s.7$ at 195λ, and $\Delta\alpha = -4^s.6 \pm 1^s.4$ at 283λ.

(51) 3C 387. Probably extended (3C). The difference between the 283λ position and that of 3C suggests that phase shifts due to resolution are present.

(52) 3C 388. The phase shift due to resolution is $\Delta\alpha = 0^s.0 \pm 0^s.4$ at 195λ, and $\Delta\alpha = 0^s.0 \pm 0^s.9$ at 283λ calculated from the model of M^2.

(53) 3C 389. 3C-R gives a diameter of 3!3 $\pm$ 2!0, suggesting that there may be phase shifts at 195λ and 283λ. However, the agreement between the positions at the two spacings suggests that any phase shifts are small.

(54) 3C 391. 3C-R gives a diameter of 2!0 $\pm$ 2!0. However, Allen et al (1962) suggest a smaller size (<1'). The disagreement between the positions at 195λ and 283λ suggests that phase shifts are probably present.

(55) 3C 396. 3C-R gives a diameter of 3!0 $\pm$ 2!0. CTB gives a diameter of 4'. A phase shift is likely at 283λ.

(56) 3C 397 = CTB 67. 3C-R gives a diameter of 3!0 $\pm$ 2!0. CTB gives a diameter of 7'. Phase shifts due to resolution are probable and seem to be present at 195λ and 283λ.

(57) M19-111. The positions given here agree with the positions derived from a drift curve, but disagree with the MSH position by 40^s.

(58) CTB 87. Galactic source with an east-west diameter of 3!8 $\pm$ 0!5 (M^2). No phase shift measurements were made by ATM; however, the agreement between the positions at 195λ and 283λ suggests that any phase shifts are small.

(59) M20-214. No size information available, but the disagreement between the 195λ and 283λ positions suggests that phase shifts are present.

Notes to Table 3 (concluded)

(60) M20-215. MSH gives size as <20". However, the disagreement between the 195λ and 283λ positions suggests that some phase shift may be present.

(61) M21-21. MSH gives a diameter >55". However, the agreement with the MSH position suggests there is probably only a small phase shift at 195λ.

(62) 3C 428. Confused by CTB 101. The effect of the confusion is not calculable.

(63) CTA 97. Large galactic source of diameter 10' ± 3' (M^2). Small but unknown phase shifts at 195λ and 283λ are probably present. No phase shift measurements were made by ATM.

(64) 3C 452. Considerable structure with an east-west diameter of $4^s.0 \pm 2^s.0$ (M^2). Phase shift likely at 195λ.

(65) 3C 461. Measured east-west phase shift by Jennison and Latham (1959) suggests very little phase shift at 195λ and 283λ. However, the phase shift becomes appreciable at the larger spacings used by 3C and ERL.

(66) 3C 465. Complex source having an overall diameter of 5!0 ± 1!0 (M^2). Detailed model not available although the agreement of the 195λ and 283λ positions suggests very small phase shifts.

Table 4

FINAL RIGHT ASCENSIONS FOR 197 SOURCES
INCLUDING KNOWN CORRECTIONS

Source	α(1950.0)	Std. Error	Remarks*
3C 2	$00^h03^m48^s.3$	±0.8	
3C 5	00 09 47.6	0.9	
M00-29	00 21 59.8	0.5	
3C 10	00 22 27.9	1.2	Tycho S.N. (1)
3C 15	00 34 29.8	0.5	
3C 17	00 35 46.1	0.8	
3C 19	00 38 12.4	0.7	
3C 18	00 38 12.8	0.9	
M00-410	00 39 45.0	0.7	
3C 20	00 40 17.8	0.7	
M00-411	00 43 54.0	0.7	
3C 23	00 49 08.3	0.7	
3C 26	00 51 35.3	0.6	
3C 27	00 52 41.2	0.8	
3C 28	00 53 09.4	0.9	
3C 29	00 54 59.2	1.1	
M01-41	01 03 05.0	0.8	
3C 32	01 05 48.3	0.5	
3C 33	01 06 13.2	0.7	
3C 34	01 07 33.3	0.7	(5)
3C 38	01 17 59.5	1.4	
3C 40	01 23 24.4	0.9	(6)
3C 43	01 27 13.8	0.5	
3C 46	01 32 32.0	1.5	
3C 47	01 33 39.5	1.3	
3C 48	01 34 49.2	0.4	
3C 55	01 54 18.3	0.5	
M01-315	01 57 58.4	0.6	
3C 62	02 13 13.3	0.5	
3C 63	02 18 22.1	0.4	
3C 66	02 19 55.7	1.4	(10)
3C 69	02 34 15.8	0.7	
M02-110	02 35 24.7	0.5	
3C 71	02 40 07.3	0.3	
3C 75	02 55 04.4	0.6	

*The numbers refer to the notes to Table 3.

Table 4 (continued)

Source	α(1950.0)	Std. Error	Remarks*
3C 78	$03^h05^m49^s.0$	±0.4	
3C 79	03 07 11.6	0.9	
CTA 21	03 16 09.2	0.4	
3C 84	03 16 29.2	0.4	Per A
3C 86	03 23 33.7	1.1	
3C 88	03 25 18.7	0.5	
CTA 26	03 36 53.6	0.5	
M03-19	03 49 09.9	0.5	
M03-212	03 49 33.4	0.8	
3C 98	03 56 11.7	0.3	
3C 99	03 58 31.6	0.5	
3C 103	04 04 35.7	0.8	
3C 105	04 04 45.0	0.5	
M04-12	04 05 30.6	1.2	
3C 109	04 10 55.7	0.5	
M04-24	04 13 54.9	0.5	
3C 111	04 15 02.1	0.7	
3C 119	04 29 07.8	0.5	
M04-112	04 31 51.4	0.5	
3C 123	04 33 55.6	0.4	
M04-218	04 42 37.7	0.5	
3C 131	04 50 11.1	0.7	(16)
3C 132	04 53 42.6	0.9	(17)
3C 133	04 59 53.7	0.6	
3C 134	05 01 18.2	0.7	
M05-42	05 11 31.4	1.0	
3C 135	05 11 33.4	1.0	(18)
3C 138	05 18 16.3	0.5	
M05-36	05 21 12.4	0.7	
3C 144	05 31 30.5	0.3	Tau A
3C 145	05 32 51.5	0.6	Ori A
3C 147	05 38 43.2	0.6	
3C 149	05 47 58.3	0.6	
3C 152	06 01 27.7	0.6	
3C 153	06 05 43.4	0.6	
3C 154	06 10 42.8	0.6	
3C 158	06 18 51.0	0.5	
3C 159	06 21 39.9	1.1	(20)
3C 161	06 24 43.1	0.7	
3C 166	06 42 24.7	0.5	

Table 4 (continued)

Source	α(1950.0)	Std. Error	Remarks*
3C 171	$06^h51^m11^s.7$	±0.8	
M06-216	06 56 53.0	0.7	
3C 172	06 59 03.2	0.5	
3C 175	07 10 14.7	0.4	
3C 178	07 22 31.7	0.6	
3C 180	07 24 33.2	0.4	
2C 665	07 31 22.6	0.7	
3C 191	08 02 01.9	1.2	
3C 192	08 02 35.6	0.5	
3C 195	08 06 30.6	0.5	
3C 196	08 10 00.1	0.5	
3C 198	08 19 52.6	0.6	
3C 200	08 24 18.6	0.6	
3C 202	08 31 56.8	0.9	(25)
3C 212	08 55 55.0	0.8	
M08-47	08 57 23.0	1.1	(27)
CTB 32	08 57 41.4	1.0	
M08-219	08 59 38.2	0.7	
3C 216	09 06 17.6	1.0	
3C 218	09 15 41.8	0.5	Hya A (29)
3C 219	09 17 51.5	0.8	
3C 222	09 33 51.5	1.2	
3C 225	09 39 31.1	0.5	
3C 227	09 45 09.4	1.0	
3C 228	09 47 28.3	0.6	
3C 230	09 49 24.0	0.7	
3C 231	09 51 45.2	1.5	
3C 234	09 58 57.3	0.7	
3C 237	10 05 18.6	0.9	
3C 238	10 08 24.9	0.7	
3C 254	11 11 54.8	1.2	
3C 264	11 42 32.3	0.9	
3C 265	11 42 53.4	0.6	
3C 270	12 16 49.9	0.4	
3C 272.1	12 22 33.0	0.6	
3C 273	12 26 33.7	0.3	
3C 274	12 28 18.4	0.5	Vir A (34)
3C 275	12 39 45.0	0.4	
3C 277.3	12 51 46.9	0.7	Com A
3C 278	12 51 58.8	0.4	(35)

Table 4 (continued)

Source	α(1950.0)	Std. Error	Remarks*
3C 279	$12^h53^m35^s.9$	±0.8	
3C 280	12 54 40.1	0.7	
3C 283	13 08 57.4	0.4	
M13-42	13 22 34.8	0.6	Cen A (36)
3C 287	13 28 15.7	0.4	(37)
3C 286	13 28 49.7	0.5	
3C 295	14 09 33.2	0.4	
3C 298	14 16 38.8	0.6	
3C 300.1	14 25 58.3	0.5	
M14+010	14 34 27.6	0.9	(40)
M14-121	14 53 12.8	0.4	
3C 309.1	14 58 53.0	1.1	
3C 310	15 02 48.5	0.3	
3C 313	15 08 33.1	0.3	
3C 315	15 11 30.8	0.4	
3C 317	15 14 18.2	0.9	
3C 318	15 17 50.0	0.4	
3C 319	15 22 44.7	1.7	
3C 321	15 29 39.0	0.6	
3C 324	15 47 37.9	0.8	(43)
3C 327	15 59 55.6	0.7	(44)
3C 327.1	16 02 13.4	0.7	
M16+03	16 03 39.5	0.6	
3C 330	16 09 15.1	0.9	
3C 332	16 15 46.0	1.0	
3C 334	16 18 07.5	0.7	
M16-18	16 21 13.5	0.5	
3C 338	16 26 54.6	0.6	
3C 345	16 41 18.4	1.3	
3C 348	16 48 41.2	0.3	Her A
3C 353	17 17 56.1	0.5	
3C 358	17 27 41.8	1.3	Kepler S.N.
M17-213	17 42 32.2	0.4	Sgr A
3C 365	17 56 12.6	1.3	
M17-217	18 00 07.1	0.7	
M18-13	18 11 17.0	0.5	
M18-33	18 17 07.4	1.2	
CTB 52	18 17 42.1	1.3	M 17 (50)
3C 380	18 28 12.2	0.7	
3C 382	18 33 12.6	0.5	

Table 4 (concluded)

Source	α(1950.0)	Std. Error	Remarks*
3C 386	$18^h36^m13^s.4$	±0.4	
3C 388	18 42 36.0	0.8	(52)
3C 390	18 43 15.2	0.5	
3C 389	18 43 44.8	0.7	
3C 394	18 57 04.9	0.5	
M19-46	19 32 17.6	0.8	
M19-111	19 38 24.8	1.7	
3C 401	19 39 38.0	0.7	
3C 402	19 40 22.5	0.6	
3C 403	19 49 43.5	0.6	
3C 405	19 57 44.5	0.4	Cyg A
3C 409	20 12 18.0	0.8	
CTB 87	20 14 10.5	0.7	
3C 410	20 18 03.9	0.5	
3C 413	20 28 25.0	1.0	
M20-37	20 32 35.6	0.5	
3C 418	20 37 06.6	0.4	
3C 424	20 45 44.4	0.5	
M20-215	20 58 39.1	1.5	(60)
M21-21	21 04 26.1	0.5	
3C 427.1	21 04 41.7	3.1	
3C 430	21 17 02.9	1.0	
3C 431	21 17 09.0	0.8	
3C 433	21 21 30.6	0.4	
3C 435	21 26 38.0	0.8	
3C 436	21 41 57.6	0.6	
3C 437	21 45 00.0	0.7	
3C 438	21 53 45.8	0.5	
3C 441	22 03 50.0	0.6	
3C 444	22 11 43.0	0.5	
3C 442	22 12 20.4	0.7	
3C 445	22 21 15.4	0.4	
3C 446	22 23 11.3	0.6	
CTA 102	22 30 07.5	0.6	
M22-46	22 50 10.2	0.9	
3C 455	22 52 36.4	1.0	
3C 456	23 09 55.5	0.4	
3C 459	23 14 02.3	0.4	
3C 461	23 21 06.8	0.8	Cas A (65)
M23-112	23 22 43.3	0.8	
M23-44	23 31 42.8	0.8	
3C 465	23 35 56.6	0.7	

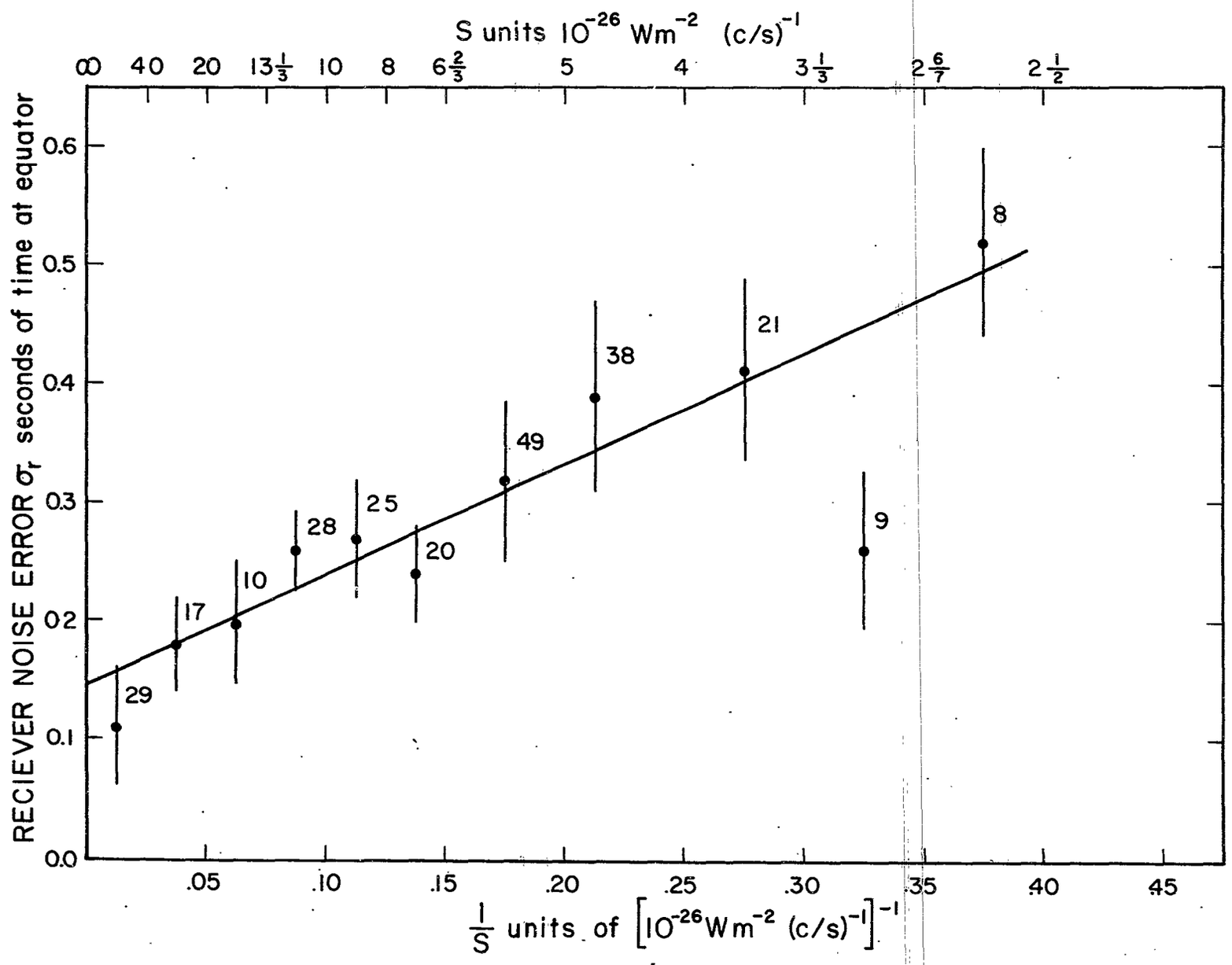

Figure 1. Receiver noise error as a function of source intensity. All the observations at 195λ (958 Mc/s) are included with the number indicating the number of sources averaged for that point. The unit of flux is in 10^{-26} W m^{-2} $(c/s)^{-1}$.

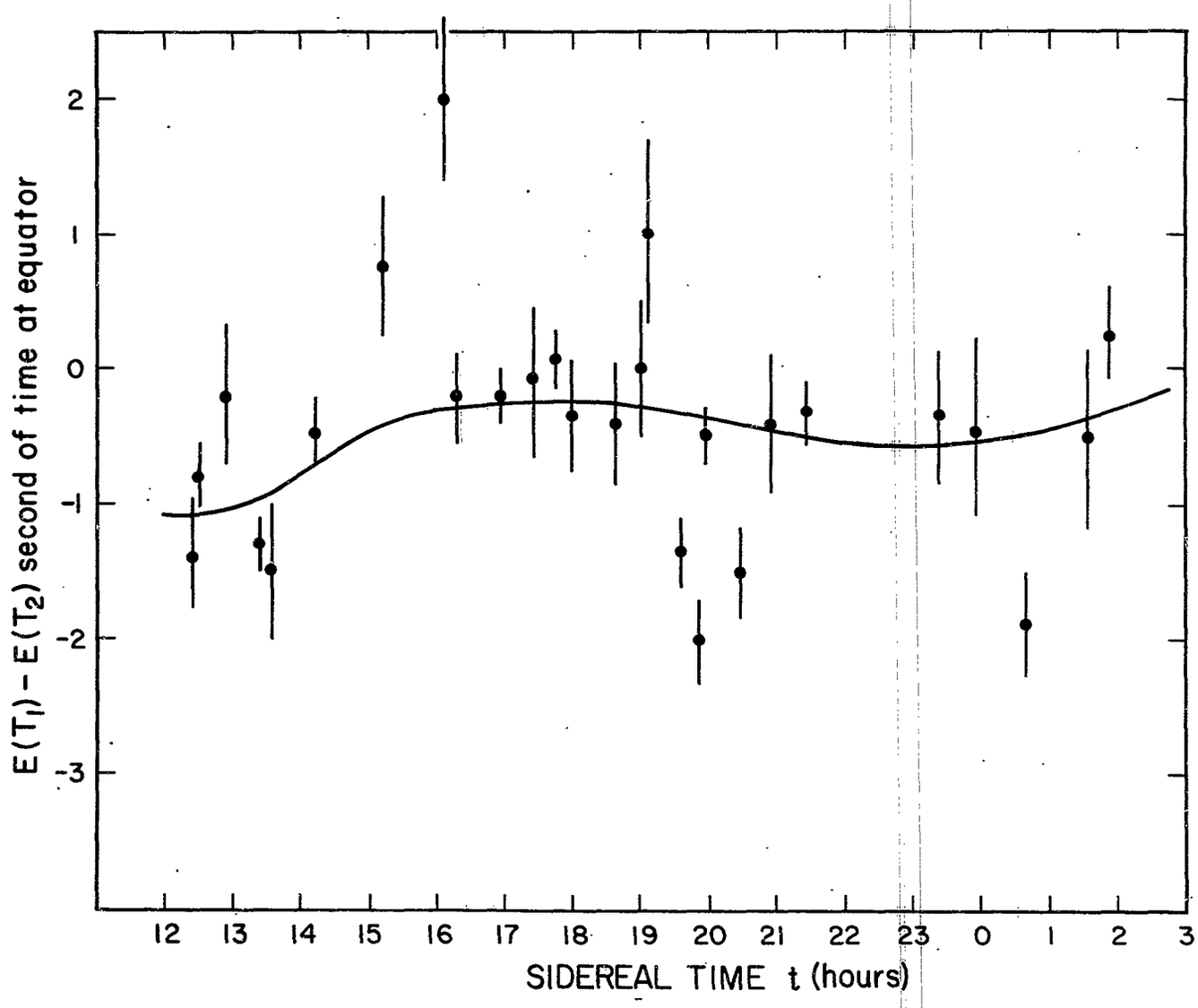

Figure 2. Transit time comparison of sources observed on July 19-20 and July 20-21, 1961. The scatter about the mean line is greater than expected from the receiver noise. The additional scatter is caused by random equipment phase jumps.

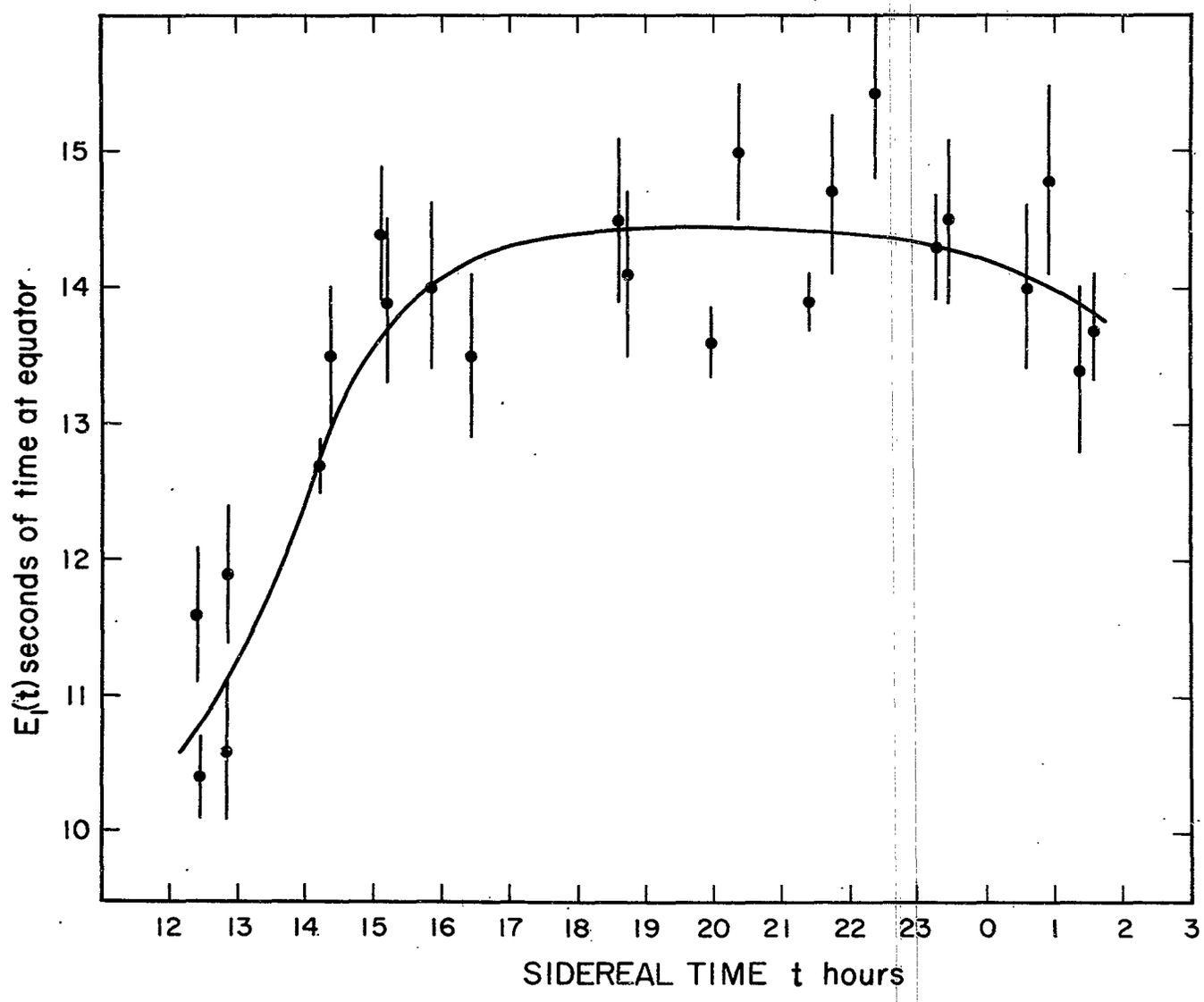

Figure 3. The final iteration for the calibration of interferometer phase $E_1(t)$ for the standard night July 19-20, 1961.

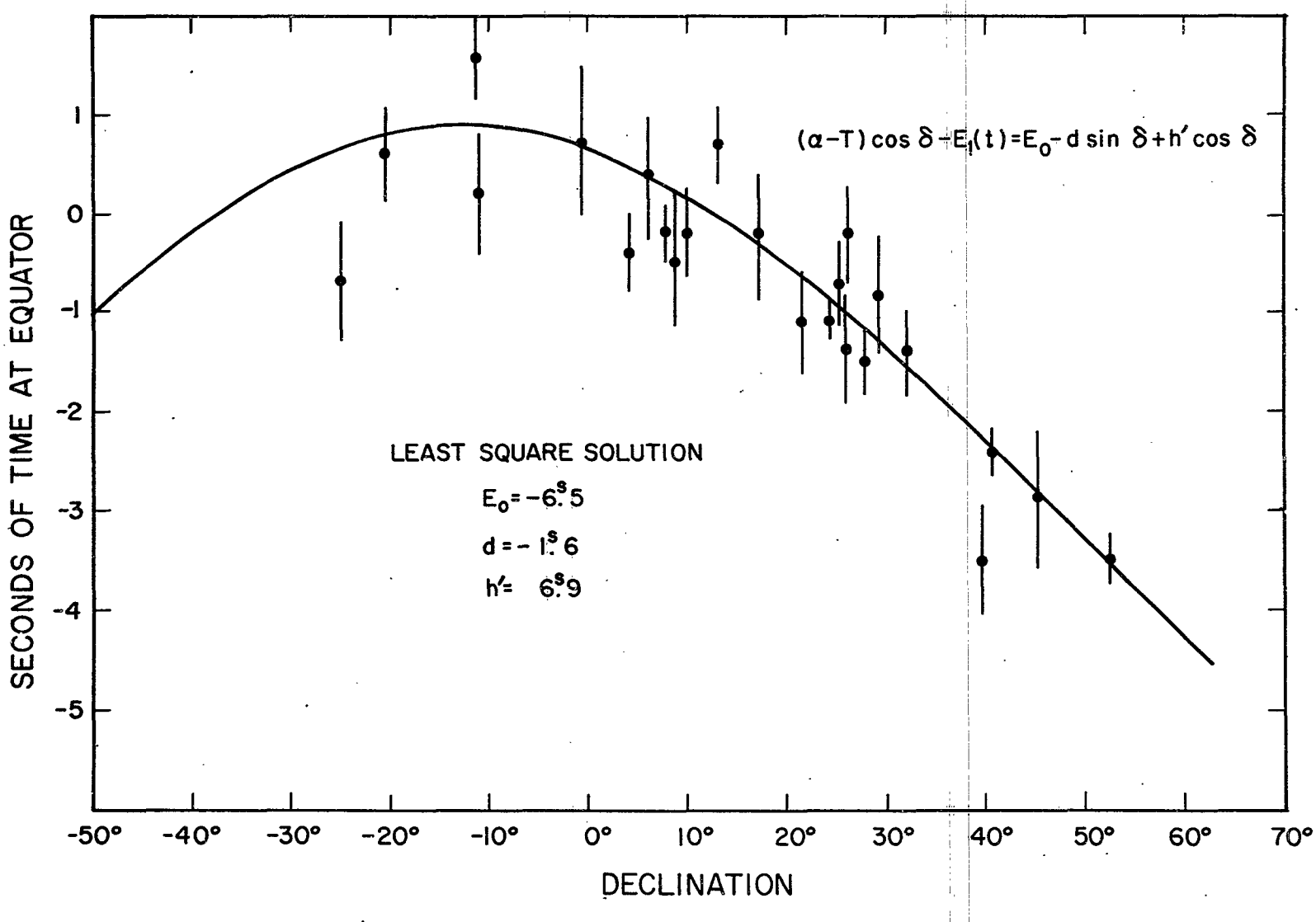

Figure 4. Base line calibration. This is the final iteration for the July 1961 series. The lack of calibrators south of declination -20° causes an additional uncertainty in this region.

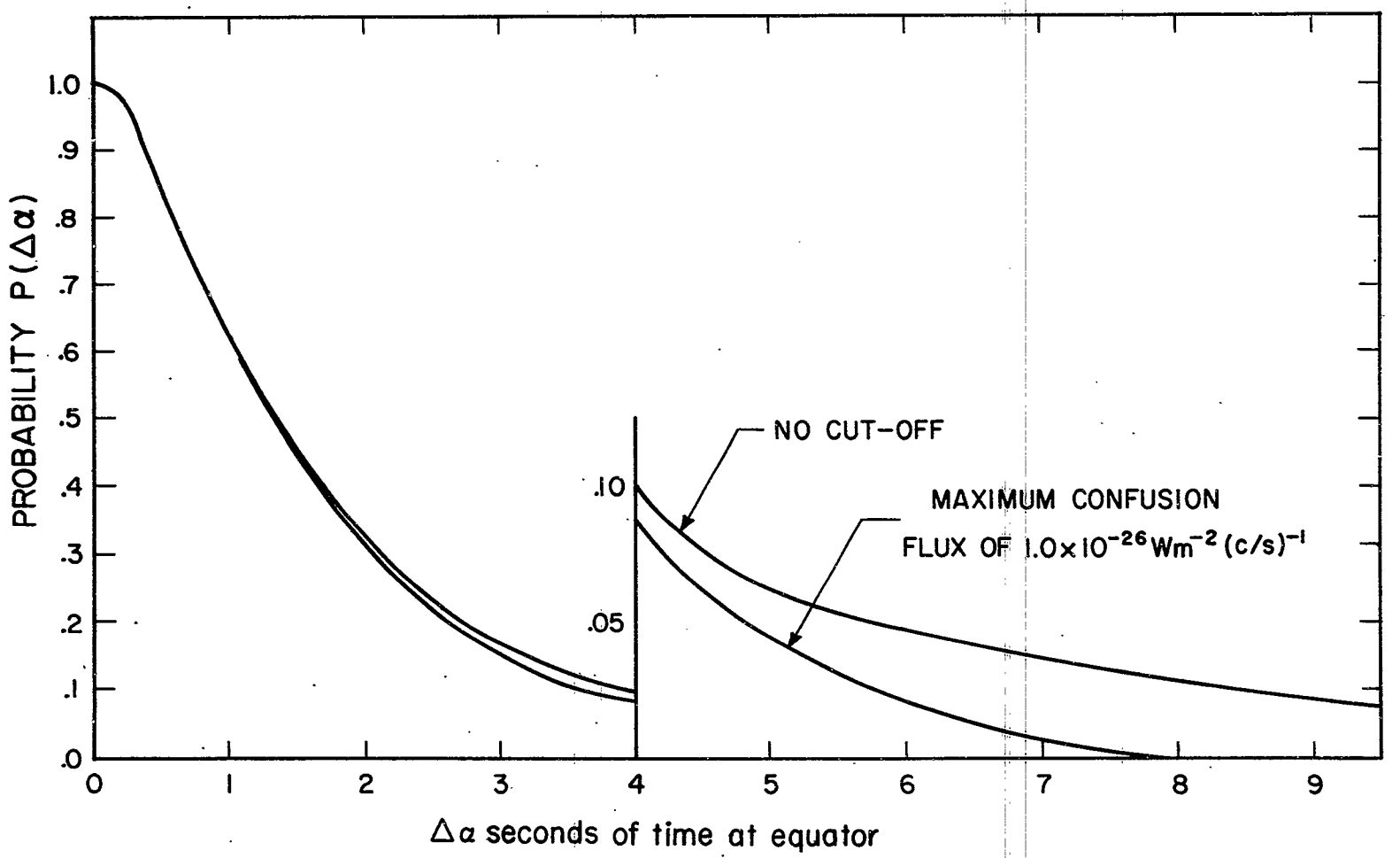

Figure 5. The effect of confusion. $P(\Delta\alpha)$ is the probability that a source of unit flux [1 x 10^{-26} W m^{-2} $(c/s)^{-1}$] will have its apparent position shifted <u>at least</u> $\Delta\alpha$ seconds of time at the equator. A source of flux S will be shifted <u>at least</u> $\Delta\alpha$ x 1/S.

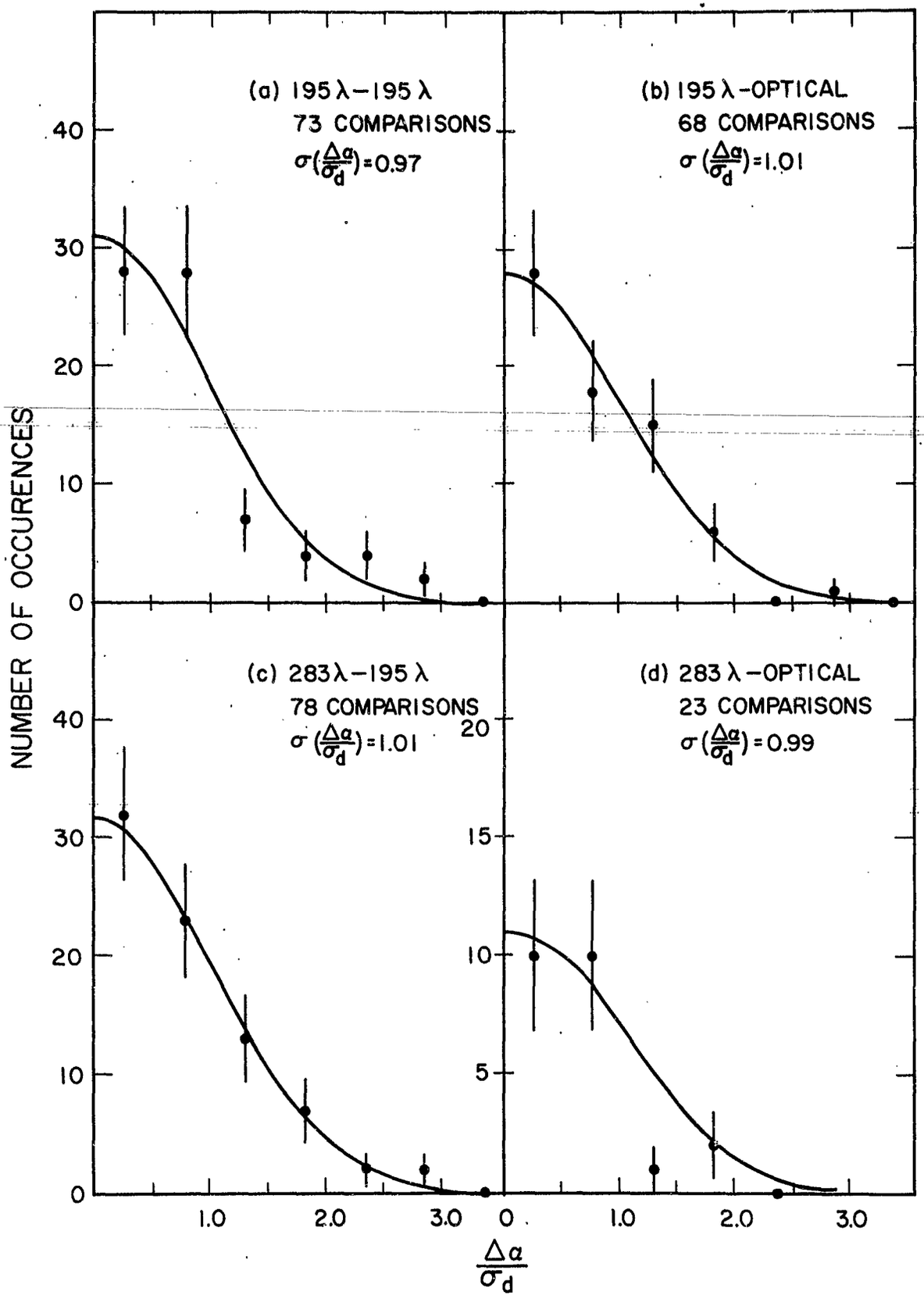

Figure 6. The comparison of the observed differences in right ascension with the expected error. For a description of the different sets of comparisons and an explanation of the method see text section V (f).